

REMOTE DETECTION AND IDENTIFICATION OF MICROBIAL HABITATS IN THE ALTIPLANO OF CHILE, A MARS ANALOG. M. S. Phillips¹, J. E. Moersch¹, K. Warren-Rhodes², N. W. Hinman³, and N. A. Cabrol². ¹Department of Earth and Planetary Sciences, University of Tennessee, Knoxville, TN 37996-1526 (mphil58@vols.utk.edu), ²SETI Institute, Moffett Field, CA, ³Department of Geosciences, University of Montana, Missoula.

Introduction: The guiding theme of Mars exploration is changing from global and regional habitability assessment to biosignature detection [1]. With this change, it is useful to focus on the reliable identification of specific *habitats* with high biosignature preservation potential [2]. Microbial habitats are often small and are at or below the spatial resolution of even the most capable Mars orbital assets, such as High Resolution Imaging Science Experiment (HiRISE, ~0.25 m/pixel) and Context Camera (CTX, ~5 m/pixel). The goal of this work is to establish thresholds of detection (the spatial resolution necessary to recognize characteristics of a target) and thresholds of identification (the spatial resolution necessary to positively identify a target) for habitats in terrestrial Mars analog environments. Such thresholds inform the search for possible paleohabitats on Mars and can guide performance objectives for future instruments.

Geologic Background: The focus of this work is on surface features within Salar de Pajonales (SdP, 25° 08' 00" S, 68° 50' 00" W, 3545 m, see Figure 1), a salt-encrusted playa (salar) in the Altiplano of Chile located between the Atacama Central Depression and the pre-Andean Cordillera de Domeyko [3]. Salars, such as SdP, are evaporitic basin environments conducive to the preservation of biosignatures, perhaps analogous to proposed chloride deposits on Mars [4].

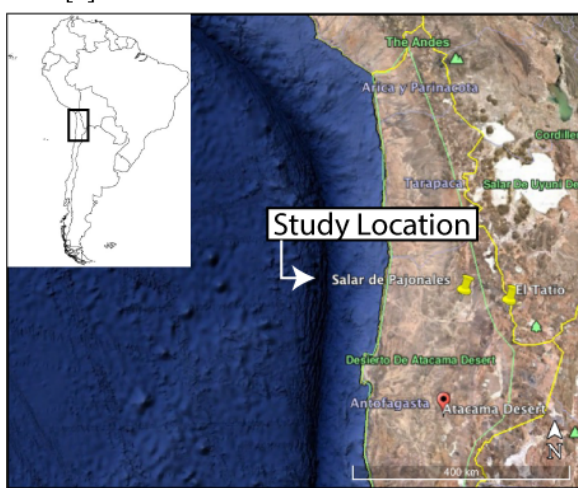


Figure 1: Location of our study area, Salar de Pajonales within South America. Image source: Google Earth.

We have defined four main surface units at our study location, Campo de Domos, within SdP: i) isolated, near-circular **domes** comprised of radial selenite, ii) sinuous **ridges** commonly connected as edges of decameter-scale polygonal networks, iii) **flat**

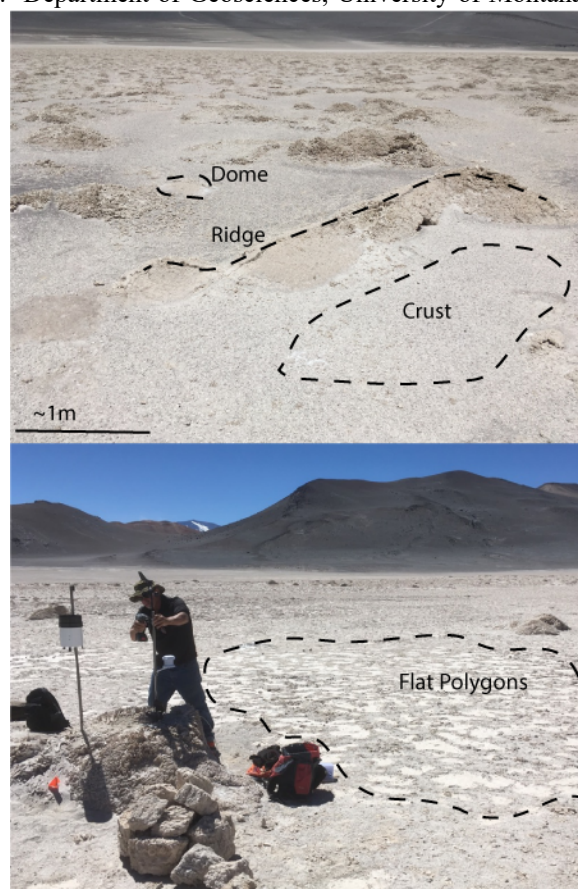


Figure 2: examples of the four surface units: crust, domes, ridges, and flat polygons.

polygons, commonly with polished surfaces, forming a mosaic of submeter-scale polygons, and iv) surficial aeolian/detrital **crust** composed of gypsum float and wind-blown volcanic sediment. Microbes colonize these units at different rates, preferring domes and ridges and the margins of flat polygons, where they form biological soil crusts [5].

Data and Methods: We used images acquired from an unmanned aerial vehicle (UAV) at a flight altitude of 11 m corresponding to a ground sampling distance (GSD) of approximately 2.4 mm/pixel. From these images, the following higher order data products were constructed: orthomosaics, digital elevation models (DEMs), slope and aspect images, and reflectance images. Reflectance is calculated based on sensor settings (e.g., ISO, shutter speed), sensor properties, and scene conditions (e.g., phase angle). Orthomosaics, DEMs, and reflectance products were created using Pix4D software. Slope and aspect images were produced in ArcGIS from DEMs. To assess the ability to detect and identify features with

increasing GSD, degraded products ranging from ~ 3 mm/pixel to 5 m/pixel were constructed in Matlab. The chosen range of GSDs encompasses those available from HiRISE and CTX [6, 7]. When appropriate, HiRISE and CTX camera models were used to create images homologous to those obtained at Mars.

All data products were imported into ArcGIS for mapping and data extraction. Sample areas 10 m by 10 m in extent were randomly selected from the Campo de Domos study location. Mapping of surface units within sample areas was done using the polygon feature tool in ArcGIS. Data were extracted from the mapped polygon areas and used to calculate parameters as defined in Table 1 for domes, ridges, flat polygons, and crust. Parameters were used to distinguish between surface units in a multivariate analysis and were chosen because each parameter represents a method for quantifying characteristics used to distinguish surface features from each other by a human analyst.

Description of Parameters: The Reflectance Parameter measures the deviation of the RI value of surface unit, i , from the mean RI value of the sample area. Similarly, the Elevation and Slope Parameters measures the deviation of the H and m values of surface unit, i , from the mean H and m values of the sample area. Compactness is defined as the ratio of the area of an object to the area of a circle with the same perimeter. A circle is used because it is the most compact shape, and compactness takes a maximum value of 1 for a circle. Roundness measures the degree to which an object approaches a circle and is relatively insensitive to irregular shape boundaries. It is defined as the ratio of the shape area to the area of a circle with the same convex perimeter, where convex

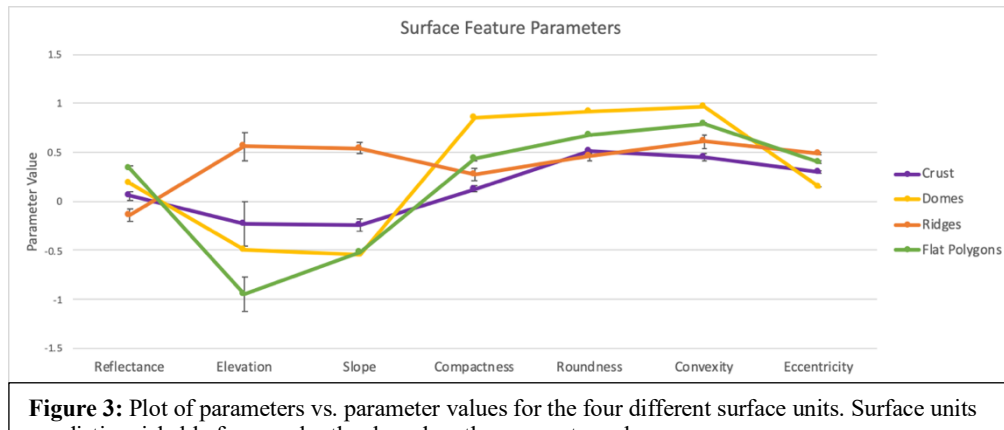


Figure 3: Plot of parameters vs. parameter values for the four different surface units. Surface units are distinguishable from each other based on the parameter values.

perimeter is the perimeter of the shape's convex hull. Convexity is the ratio of the convex perimeter to the perimeter and measures the degree to which a shape is convex. Lastly, Eccentricity measures how elliptical a shape is based on the ratio of the minor axis to the major axis of a minimum bounding ellipse.

Results: Parameter values calculated for the four surface units (crust, domes, ridges, and flat polygons) are reported in Figure 3. In general, for any two surface units the difference between parameter values is larger than the sum of their standard deviations (shown as error bars in Fig. 3), indicating the units are distinguishable from one another.

Similar analyses will be carried out at a range of GSDs to establish the GSDs at which surface units are no longer distinguishable from the average image values (threshold of detection) and from each other (threshold of identification).

Reference: [1] Mustard, J.F., et al. (2013) *Report of the Mars 2020 SDT*. [2] Cabrol N. (2018) *Astrobiology*. [3] Chong-Diaz, G. (1988) *The Southern Central Andes. Lecture Notes in Earth Sciences*. [4] Osterloo, M.M., et al. (2008) *Science*. [5] Warren-Rhodes, K., et al. (2019) *AbSciCon*. [6] McEwen, A.S., et al. (2007) *JGR: Planets*. [7] Malin, M. C., et al. (2007) *JGR: Planets*.

Acknowledgements: This research is supported by NASA Astrobiology Institute's Grant No. NNX15BB01A, "Changing Planetary Environment and the Fingerprints of Life", SETI Institute NAI team (N. A. Cabrol, P.I.)

Table 1: Equations used to calculate parameters and explanation of variables.

Reflectance Parameter	$\frac{\bar{RI}_i - \bar{RI}_{SA}}{\sigma_{RI,SA}}$
Elevation Parameter	$\frac{(\bar{H}_i - \bar{H}_{SA})}{\sigma_{H,SA}}$
Slope Parameter	$\frac{\bar{m}_i - \bar{m}_{SA}}{\sigma_{m,SA}}$
Compactness	$\frac{4\pi * A_i}{P_i^2}$
Roundness	$\frac{4\pi A_i}{P_{ci}^2}$
Convexity	$\frac{P_{ci}}{P_i}$
Eccentricity	$1 - \frac{L_{mi}}{L_{Mi}}$

\bar{RI}_i = mean reflectance index value of surface unit i .

\bar{RI}_{SA} = mean reflectance index value of sample area.

$\sigma_{RI,SA}$ = standard deviation of sample area RI values.

\bar{H}_i = elevation of surface unit, i .

\bar{H}_{SA} = mean elevation of the sample area.

$\sigma_{H,SA}$ = standard deviation of sample area H values.

A_i = area of surface unit, i .

P_i = perimeter of surface unit, i .

P_{ci} = convex perimeter of surface unit, i .

L_{mi} = minor axis of surface unit, i .

L_{Mi} = major axis of surface unit, i .